Journal of Biomolecular Structure & Dynamics, ISSN 0739-1102
Volume 27, Issue Number 3, (2009)

Ultrasonic Cleavage of Nicked DNA

http://www.jbsdonline.com

I.A. Il'icheva[1]
D.Yu. Nechipurenko[2]
S.L. Grokhovsky[1,*]

[1]Engelhardt Institute of Molecular Biology RAS, Vavilov str. 32 Moscow 119991, Russia
[2]Dep. of Physics Moscow State University Moscow 119992, Russia

Abstract

Structural properties of nicked dsDNA have been an object of numerous studies due to their special role in reparation processes. Here we report experimental results covering ultrasound irradiation of a nicked dsDNA fragments. We have quantitatively estimated ultrasonic cleavage rates in these fragments using the polyacrylamide gel electrophoresis. Data reveal cleavage enhancement in the regions of about 10 b. p. up and down the nick. The intensity of ultrasonic cleavage near the nick is one order of magnitude higher than intensity of ultrasonic cleavage in the same sites of the intact dsDNA fragments. At the same time, the cleavage rates in positions beyond the regions around the nick markedly grow weak comparing to the sequence-specific cleavage rates of intact dsDNA. Thus, the presence of the nick serves as an expressive structural alteration which exceeds any modulation of the structure caused by the base-pair sequence.

Key words: Ultrasonic cleavage of DNA; Nicked DNA; Structural dynamics of nicked DNA.

Introduction

Single-stranded DNA breaks represent the most common damage in DNA which occurs naturally in living cells. These sites in DNA are being specifically recognized by the reparation complexes, what makes studying their structural properties crucial for understating mechanisms of DNA reparation.

Ultrasonic exposure of intact DNA fragments in solution results in sequence specific cleavage which reflects structural heterogeneity of double-stranded DNA (1,2). We attribute this cleavage to the hydrodynamic shearing forces which originate from high velocity gradients in microjects caused by vibration and collapse of cavitation bubbles (3). Ultrasonic cleavage patterns of DNA support this idea by several specific features. The properties of cleavage damping observed in terminal regions of DNA fragment give evidence to the large-scale reaction of DNA to external shearing stress which involves several tens of base-pairs. In addition the intensities of bands on the gel reflect the comparative sequence specific cleavage rates of the corresponding sugar-phosphate bonds. Thus, the ultrasonic cleavage pattern seems to reflect both local and larger-scale dynamical properties of DNA molecule.

Data of X-ray analysis (4), NMR (5, 6) and molecular dynamic studies (5, 7), as well as pulsed EPR spectroscopy combined with site-directed spin labeling (8), gives consistent evidence of enhanced flexibility of the nicked site but only a small changes of 3D structure comparing to intact DNA. Only tiny decrease of electrophoretic mobility of nicked dsDNA fragments were observed at ambient temperature and without addition of DNA denaturing reagent. But in the presence of urea

*Phone: 499 135 97 18
Fax: 499 135 14 05
E-mail: grok@imb.ac.ru

the decrease of mobility became more pronounced (9,10). It may be attributed to a bend (or hinge) in the DNA double helix sequence specifically generated by a nick (9, 10). The V-like structure of the nicked DNA fragment was observed in dark-field electron microscope (11). Moreover, single-nucleoside gap in a DNA duplex leads to an anisotropic, directional bend in DNA helix axis (12). Thus, instead of the increased flexibility of the structure, nick may produce sequence specific bending of intact strand which is more pronounced in the presence of denaturing agents.

Ultrasonic cleavage analysis covers cleavage properties of DNA fragments with lengths of several hundreds of base pairs. Thus, this method might elucidate structural properties of nicked DNA fragments which become apparent on this scale and may not be accessed by NMR analysis and MD simulation.

Materials and Methods

The Restriction Fragments of DNA

The restriction fragments of DNA were generated by digestion modified analogs of plasmid pGEM7(f+) (Promega), which contained different insertions into polylinkers by the corresponding restriction endonucleases. The fragments were 3'-end-labelled with [a-^{33}P]dATP or [a-^{32}P]dATP ("FGUP" Institute of reactor materials, Zarechnii, Sverdlovskaya oblast, Russia) in the presence of the unlabeled other dNTP and the Klenow fragment of Escherichia coli DNA-polymerase I (SibEnzyme, Novosibirsk, Russia). The DNA fragments were isolated by non-denaturing PAAG in 1 mm thick 5% gel with subsequent elution and precipitation. Gels were run for 3 h at 12.5 V/cm in TBE buffer (90mM Tris-borate, 2mM EDTA, pH 8.6).

The fragments' base pair sequences and other supplementary materials can be accessed http://grok.imb.ac.ru/nick/.

Treatment of DNA Fragments with Nicking Endonuclease

The DNA fragments were incubated at 55°C with nicking endonuclease N.Bst9I (13) in volume of 30 mkl in the reaction buffer recommended by the supplier. Typically, incubation was performed for 1 h with 1-2 U of nicking endonuclease and separation in the PAAG under above conditions. Nicked fragments showed a noticeable retardation in comparison with the unaffected DNA fragments.

The Irradiation of DNA Fragments by Ultrasound

10 mkl of DNA labelled fragments in water (approximately 10^4 Bq) were mixed with 10 mkl of 0.2 M NaOAc, pH 6.0 in the bottom of thin-walled polypropylene test-tube of 0.2 ml capacity (N801-0540, Perkin-Elmer, USA). The final concentration of fragment was 5-10 mkg/ml (or ~10mkM bp).

The test-tubes were placed in teflon ring which had a central circular slot of 15 mm in diameter and the radial circular slots for the test-tubes. The test-tubes ends were located about 0.5 cm below the irradiator edge, which had the diameter of 12 mm. The ring and irradiator were placed in a vessel with water and crushed ice. Ultrasound was generated by a 300 W generator UZDN-2T (Ukraine) with a frequency of 22 kHz under maximal power condition of device.

The Separation of DNA Fragments in Denaturing Gel

After sonication the samples were combined with 180 mkl of solution of 0.15 M NaCl, 50 mM Tris-HCl (pH 7.5), 10 mM EDTA. The samples were then extracted

with phenol, DNA was precipitated with ethanol, washed with 70% ethanol, then dried and dissolved in 1.5 mkl of 95% formamide, which contained 15 mM EDTA (pH 8.0), 0.05% bromphenol blue and 0.05% xylencyanol FF, heated for 1 minute at 90°C, rapidly cooled down to 0°C and applied on the denaturing PAAG of 40 cm length and gradient width of 0.15-0.45 mm.

Electrophoresis was carried out for 55 minutes (100 Wt, 2500 V) at 60-70°C. Afterwards, the gel was fixed in 10% acetic acid and dried on to the glass plate, pretreated with γ-methacrylpropyloxysilane (LKB, Sweden). Dried gel was exposed to luminescent screen with consequent scanning by "Cyclone Storage Phosphor System" device (Packard BioScience Company, USA). Cleavage pattern bands were assigned to particular nucleotide sequences of fragments by comparison to lanes of A+G track DNA samples.

Gel Analysis

To analyze the gels we used the SAFA software, developed by scientific group in Stanford University (14). This program is capable of gel's lanes alignment, calculating the overall intensity of each band and correlation of the band sequence with corresponding base pair sequence.

Results

Figure 1 shows cleavage pattern of the strand, complementary to twice nicked strand in double-stranded DNA fragment with initial length of 253 base pairs. Two regions of cleavage enhancement are well distinguished on the picture. The most pronounced of them is disposed between positions 146 and 166, and the less pronounced - between positions 197 and 205, that is closer to the terminal part of the fragment.

Figure 2 represents band intensity data for gel presented on Figure 1. The local maximums of cleavage intensities are disposed in front of the nicks (156 and 202). Both regions of cleavage enhancement spread about 10 b. p. around the nick and their amplitudes depend on the nick distance from the ends of double-stranded DNA fragment, according to the cleavage dumping effect described in (1, 2). The maximum cleavage intensity values of nicked DNA are one order of magnitude higher than corresponding values obtained for intact DNA fragments (compare with Figure 3 - the pattern of cleavage intensities of the same strand obtained by ultrasonic irradiation of primarily intact dsDNA fragment). Cleavage intensities outside the region of the nick grow weak and reach the minima on the distance of about 30 nucleotides away from the nick position. This region of the labeled strand is characterized by cleavage rates which are markedly lower comparing to ultrasonic cleavage intensities of intact dsDNA fragments (compare Figure 2 with Figure 3). On the Figure 3 the sequence-specificity of the band intensities described in (2) is well distinguished. Consistent remarkable enhancement of cleavage rates is found in the steps with 5'-ward cytosine.

Figure 4 represents averaged band intensities in the regions around the nicks obtained by averaging the cleavage data for 20 lanes on 5 different gels with

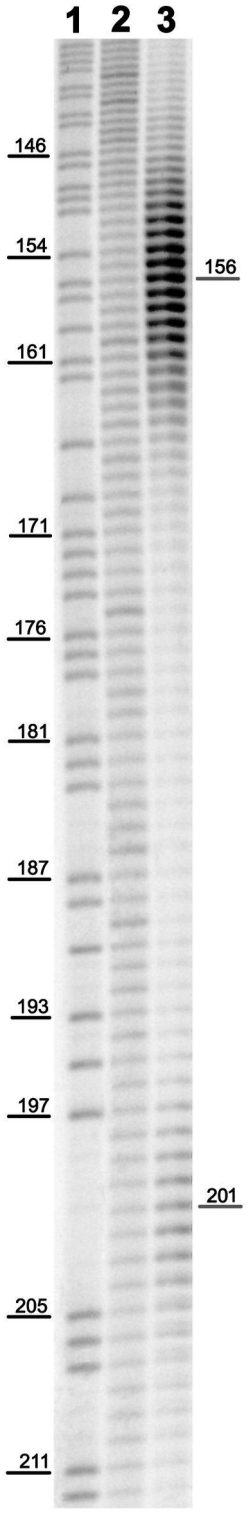

Figure 1: Cleavage pattern of dsDNA restriction fragments.
The initial length of DNA fragment was 253 base pairs. The band numeration is given from 5' - to the 3' -end of the labeled strand. Every band represents fragments of particular length which formed as a result of breakage in corresponding phosphodiester bond. The positions of initial nicks in complementary strand are given at the right side of the lane.
Lane 1 corresponds to chemical cleavage of the dsDNA fragment by the purines. Lane 2 represents ultrasonic cleavage pattern of primarily intact dsDNA fragments after irradiation for 2 min. Lane 3 shows cleavage pattern for twice nicked dsDNA fragments under the same condition with lane 2.

Figure 2: Ultrasonic cleavage intensities profile for twice nicked dsDNA fragment.
Figure plots band intensity data for lane 3 of the gel presented on Figure 1.
Each column corresponds to cleavage intensity *(y — axes)* of the phosphodiester bond which follows the nucleotide shown under the column (x - *axes).* The recognition site of N.Bst9I endonuclease is marked by the bold "GACTC" sequence, while the cleavage sites are marked by the bold "AA" and "CT" sequences and using the vertical arrow.

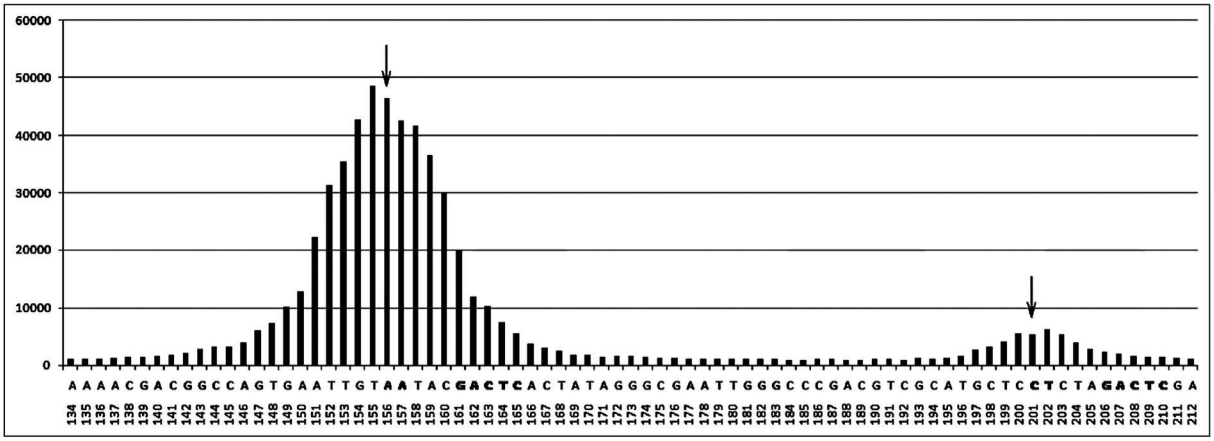

various sequences. It shows small decrease of cleavage intensity for step which is complementary to the nicked one (position "-1").

These specific features of ultrasonic cleavage of nicked DNA fragments are shown on Figure 5 in details. It represents ultrasonic cleavage patterns for intact (lane 1) and nicked (lane 2) dsDNA obtained in another experiment. The dark region of the second lane corresponds to sharp cleavage enhancement due to the nick in complementary strand. This region is conditionally marked by the first selection bar. The second selection bar corresponds to the region with low cleavage rates - where the cleavage pattern is faintly observable and the values of band intensities are much smaller than the corresponding values for intact dsDNA fragments in lane 1. Beyond this region the cleavage rates of nicked DNA gradually reach the cleavage intensity values almost identical to corresponding values for intact dsDNA fragments - with likely the same sequence-specific cleavage pattern. This region is conditionally marked by selection bar "III" with arrow pointing down and might be roughly characterized by the distances of more than 50 nucleotides from the nick.

Figure 6 represents two cleavage patterns of the primarily intact strand of nicked dsDNA fragments. Lane 1 represents ultrasonic cleavage pattern of nicked dsDNA fragment without urea in the solution, while lane 2 corresponds to cleavage pattern of nicked dsDNA in 2M urea solution. The band intensities of both lanes are identical.

Figure 3: Ultrasonic cleavage intensities profile for primarily intact dsDNA fragment.
Figure plots band intensity data for lane 2 of the gel presented on Figure 1.
Each column corresponds to cleavage intensity *(y — axes)* of the phosphodiester bond which follows the nucleotide shown under the column *(x — axes).* The remarkable enhancement of cleavage is seen in the5'-CpG-3' steps.

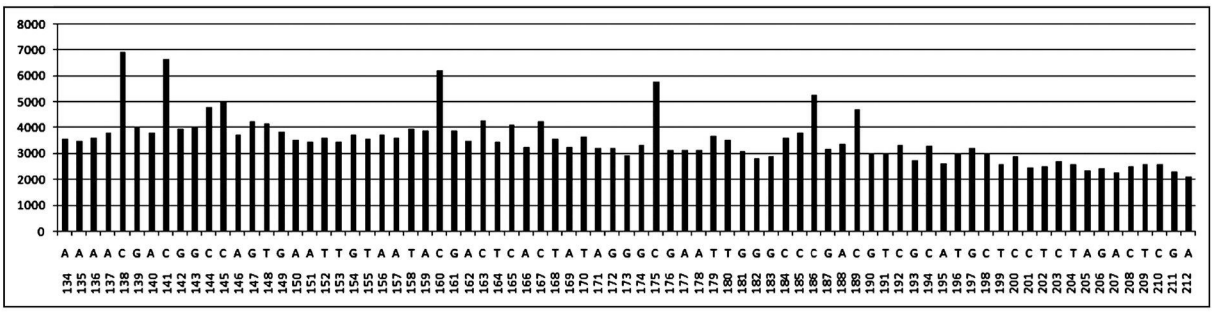

What is a sense of the bell-shaped enhancement of the ultrasonic cleavage in complementary strand in front of the nick? At least two special structural features of dsDNA near the nick site may influence the cleavage properties, namely V-shaped bending of DNA axis (9-11) and the increase of flexibility around the nick (4-8). Really, in our experiments in agreement with (9-10) nicked fragments showed retardation in comparison with the unaffected DNA fragments (see materials and methods). A more significant retardation of a nicked DNA fragment was observed in the presence of urea. It intensified dsDNA structural distortions at the nicked site (9,10). But ultrasonic cleavage patterns of nicked dsDNA fragment obtained in the presence of urea were identical to that without urea (Figure 6).

Thus, the registered splash of ultrasonic cleavage intensity around the nick might be a result of enhanced flexibility of the structure. Correlation between enhancement of structural flexibility around the nick in dsDNA and the remarkable increase of its cleavage upon ultrasound irradiation resemble the data on sequence specific ultrasonic cleavage in intact dsDNA fragments (2). All steps with 5'-ward cytosine show the remarkable enhancement of ultrasonic cleavage in respect to the other steps (2). At the same time, combined NMR ^{13}C spin relaxation data and MD simulation study evidenced, that for the cytosine deoxyribose moiety in B-DNA repuckering is a likely motional model and C-H vectors in all cytosine deoxyribose moieties are subject to high amplitude motions, while the other nucleotides are essentially rigid in this term (15). Hence, we assume that the increased flexibility of nicked dsDNA leads to observed ultrasonic cleavage rate enhancement in the corresponding regions of the labeled strand.

In conclusion, the presence of the nick leads to expressive alteration of the local dynamical properties of DNA fragments which exceeds modulation of the structural properties caused by the base-pair sequence and shows itself on the scales of several tens of base pairs. It seems that remarkable enhancement of local flexibility

Figure 4: Average ultrasonic cleavage profile of nicked dsDNA fragments.
Figure plots averaged cleavage profile of the labeled strands which were complementary to primarily nicked strands.
20 different lanes of 5 different gels were used for the averaging. Different gels correspond to ultrasonic cleavage experiments carried out with DNA fragments of different sequences. For each cleavage profile the region of 50 bands around the nick was selected. Then the band intensities were normalized by dividing their values by the average band intensity value of this 50 bands region. Consequently, all of 20 normalized cleavage profiles were summed up to give the average profile. Column marked by "-1" value on the x-axes corresponds to average relative cleavage rate of the phophodiester bond which is opposite to the primarily nicked one. Next column, marked by the value "1", corresponds to average relative cleavage rate of the next phophodiester bond while moving towards the 3'-end of the labeled strand, etc.

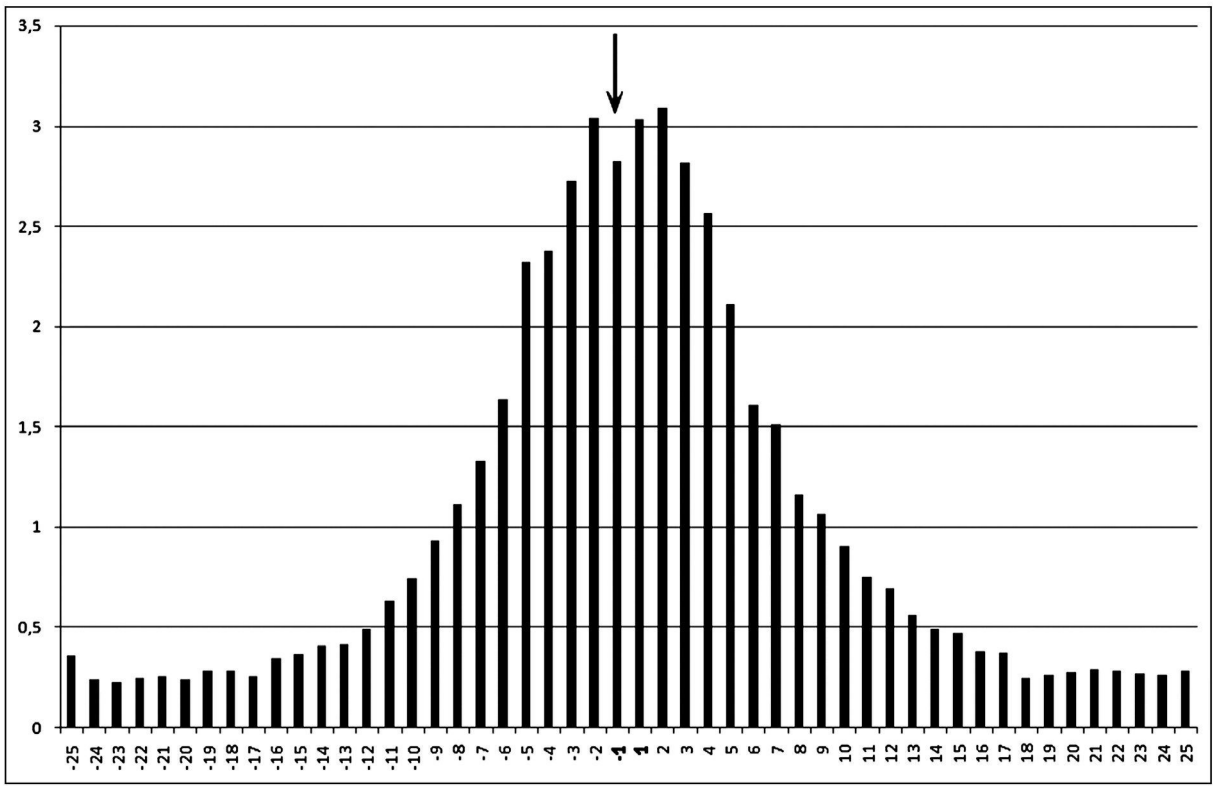

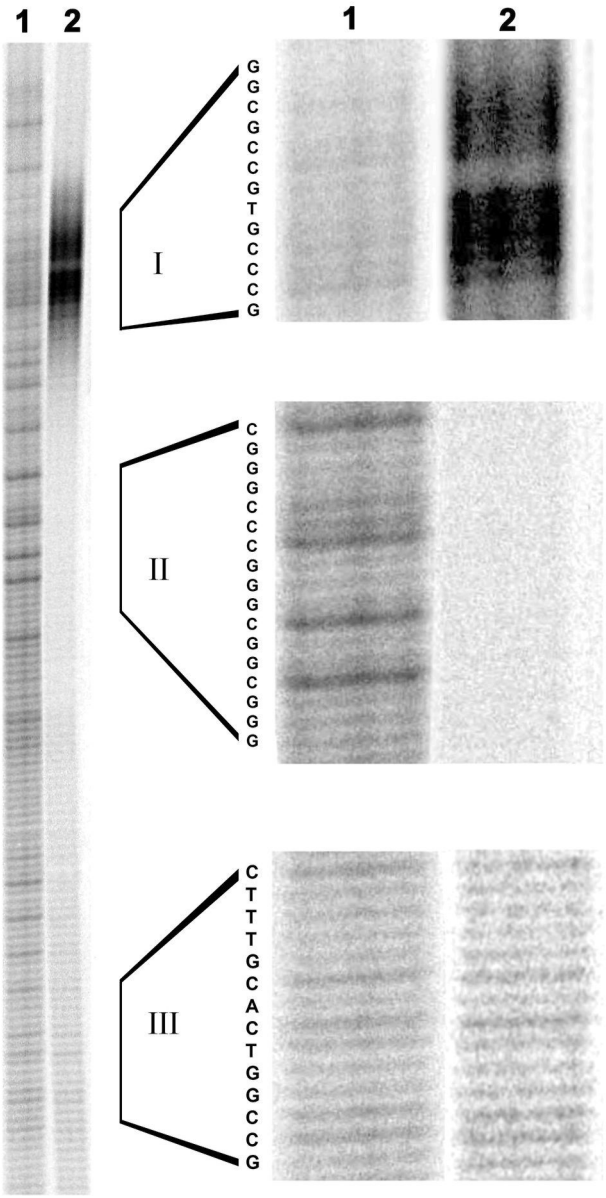

Figure 5: Specific features of ultrasonic cleavage profile of nicked DNA fragments.
Two lanes of the gel are shown for comparison. The first lane corresponds to ultrasonic cleavage of intact dsDNA fragment, while the second one corresponds to the nicked DNA. The initial fragment's length was 342 b p.
Three selected regions of the second lane demonstrate large scale heterogeneity of the cleavage pattern for nicked DNA fragment comparing to intact dsDNA. All of the regions for both lanes are shown at the zoomed level to the right side of the figure along with the corresponding sequence.
Dark bands in the first lane correspond to cleavage enhancement at the phosphodiester bond following the 5'-cytosine. The third region in both lanes looks fainted due to the cleavage dumping effect which shows itself at the terminal sites of the fragment.

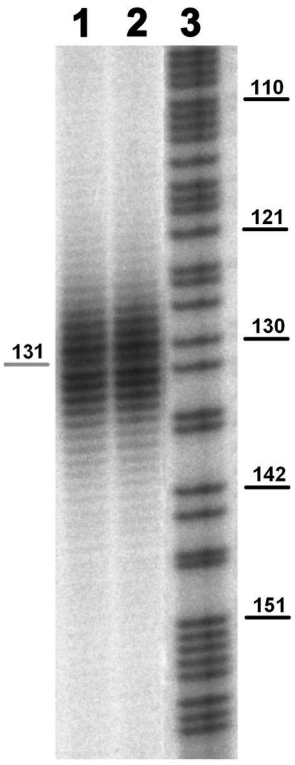

Fig. 6: Cleavage pattern of nicked DNA in presence of urea
The initial length of DNA fragment was 226 base pairs.
Lane 1 shows ultrasonic cleavage pattern of nicked DNA fragments without urea. The position of initial nick in complementary strand is given at the left side of the lane. Lane 2 represents ultrasonic cleavage pattern of nicked DNA fragments in 2 M urea solution. Lane 3 corresponds to chemical cleavage of the dsDNA fragment by the purines.

of sugar phosphate backbone around the nick is the main course of the observed cleavage pattern.

Acknowledgments

This study was supported by the Program of the Presidium of the Russian Academy of Sciences on Molecular and Cell Biology and Russian Foundation for Basic Research (projects 08-04-01739 and 07-04-01031).

References and Footnotes

1. S. L. Grokhovsky. *Molecular Biology (Russia, translated) 40,* 276-283 (2006).
2. S. L. Grokhovsky, I. A. Il'icheva, D. Yu. Nechipurenko, L. A. Panchenko, R. V. Polozov, and Yu. D. Nechipurenko. *Biophysics (Russia, translated) 53,* 208-209 (2008).
3. N. J. Pritchard, D. E. Hughes, and A. R. Peacocke. *Biopolymers 4,* 259-273 (1965).
4. J. Aymami, M. Call, G. A. van der Marel, and J. H. van Boom. *Proc Natl Acad Sci U.S.A. 87,* 2526-2530 (1990).
5. C. Roll, Ch. Ketter, V. Faibis, G. V. Fazakerley, and Y. Boulard. *Biochemistry 37,* 4059-4070 (1998).

6. J. M. L. Pieters, R. M. W. Mans, H. van den Elst, G. A. van der Marel, J. H. van Boom, and *C. Altona. Nucleic Acids Res 17,* 4551-4565(1989).
7. H. Yamaguchi, J. G. Siebers, A. Furukawa, N. Otagiri, and R. Osman. *Radiation Protection Dosimetry 99,* 103-108 (2002).
8. G. Sicoli, G. Mathis, S. Aci-Seche, C. Saint-Pierre, Y. Boulard, D. Gasparutto, and S. Gambarelli. *Nucleic Acids Res, doi:10.1093/nar/gkp165,* (2009).
9. H. Kuhn, E. Protozanova, and V. Demidov. *Electrophoresis 23,* 2384-2387 (2002).
10. E. Protozanova, P. Yakovchuk, and M. D. Frank-Kamenetskii. *J Mol Biol 342,* 775-785 (2004).
11. E. Le Cam, F. Fack, J. Menissier-de Murcia, J. A. Cognet, A. Barbin, V. Sarantoglou, B. Revet, E. Delain, and G. de Murcia. *J Mol Biol 235*, 1062-1071 (1994).
12. H. Guo and T. D. Tullius. *PNAS 100,* 3743-3747 (2003).
13. V. S. Dedkov, M. A. Abdurashitov, N. K. Yankovsky, E. V. Kileva, T. V. Myakisheva, D. V. Popichenko, and S. Kh. Degtyarev. *Biotehnologia (Russia) 4,* 3-8 (2001).
14. R. Das, A. Laederach, S. M. Pearlman, D. Herschlag, and R. B. Altman. *RNA 11,* 344-354 (2005).
15. E. Duchardt, L. Nilsson, and J. Schleucher. *Nucleic Acids Res* 36, 4211-4219 (2008).

Date Received: June 19, 2009

Communicated by the Editor Valery Ivanov